Natural marine seepage blowout: Contribution to atmospheric methane

Ira Leifer,[1,2] Bruce P. Luyendyk,[2,3] Jim Boles,[3] and Jordan F. Clark[3]

[1] The release of methane sequestered within deep-sea methane hydrates is postulated as a mechanism for abrupt climate change; however, whether emitted seabed methane reaches the atmosphere is debatable. We observed methane emissions for a blowout from a shallow (22 m) hydrocarbon seep. The emission from the blowout was determined from atmospheric plume measurements. Simulations suggest a 1.1% gas loss to dissolution compared to ~10% loss for a typical low-flux bubble plume. Transfer to the atmosphere primarily was enhanced by the rapid upwelling flows induced by the massive discharge. This mechanism could allow methane suddenly released from deeper (>250 m) waters to contribute significantly to atmospheric methane budgets.

Citation: Leifer, I., B. P. Luyendyk, J. Boles, and J. F. Clark (2006), Natural marine seepage blowout: Contribution to atmospheric methane, *Global Biogeochem. Cycles*, *20*, GB3008, doi:10.1029/2005GB002668.

1. Introduction

[2] Atmospheric methane, CH_4, is the most abundant organic compound in the atmosphere and an important greenhouse gas at least 20 times more potent than carbon dioxide, CO_2 [*Khalil and Rasmussen*, 1995]. Its atmospheric mixing ratio has more than doubled during the last century [*Rowland*, 1985]. CH_4 has both anthropogenic ($360-430$ Tg yr^{-1}; 1 Tg = 10^{12} grams) and natural sources ($160-240$ Tg yr^{-1}) of either biologic or geologic origin [*Intergovernmental Panel on Climate Change (IPCC)*, 2001; *Kvenvolden and Rogers*, 2005; *Prather et al.*, 1995]. Ranges of emission estimates are large, because as recently outlined by *Reeburgh* [2003], numerous problems arise when quantifying sources and sinks within the CH_4 budget.

[3] *Kvenvolden and Rogers* [2005] estimate that the natural geologic source to the atmosphere from both marine and terrestrial reservoirs is 45 Tg yr^{-1}. One of the contributing reservoirs is marine seepage associated with hydrate dissociation and leakage from deeper hydrocarbon reservoirs. The contribution of these seafloor sources to atmospheric CH_4 is uncertain due to the likelihood that some or all of the emitted CH_4 dissolves into the ocean during transit from the seabed to the sea surface [*Clark et al.*, 2003; *Heeschen et al.*, 2003; *Leifer and Judd*, 2002]. Global emission estimates for marine seeps (neglecting methane hydrates) are $\sim10-30$ Tg yr^{-1} [*Kvenvolden et al.*, 2001] or $\sim13\%$ of natural emissions. Although seeps exist on all continental shelves [*Hovland et al.*, 2002], few quantitative

emission rates have been published [e.g., *Hornafius et al.*, 1999]; thus the estimate is poorly constrained.

[4] Seepage emission estimates are mostly based on observations of gentle bubble emanations [e.g., *Hornafius et al.*, 1999; *Dimitrov*, 2002; *Washburn et al.*, 2005]; however, features in marine sediments [*Hovland et al.*, 2002] and underlying rock structures [*Loseth et al.*, 2001] preserve widespread evidence indicative of blowout events (eruptions) that suddenly released large amounts of gas. Because the magnitude and frequency of these large events remains unknown, their contribution to seepage emissions is unquantified.

[5] Methane hydrate dissociation may play an important role in atmospheric CH_4 budgets and climate change [*Dickens et al.*, 1995; *Katz et al.*, 1999; *Kennett et al.*, 2003; *Norris and Röhl*, 1999; *Severinghaus et al.*, 1998]; however, dissolution in the water column presents a formidable barrier to hydrate CH_4 reaching the atmosphere in the tropics and midlatitudes [*Leifer and Patro*, 2002; *MacDonald et al.*, 2002]. Here the timescale for microbial CH_4 oxidation in the deep-sea is ~1 year [*Watanabe et al.*, 1995; *Valentine et al.*, 2001], which is short compared to the timescale to diffuse to the winter mixed-layer, ~50 years [*Rehder et al.*, 1999].

[6] Herein we present the first quantitative observations of a large, blowout seepage-event and associated bubble plume processes along with a numerical study of the event. We conclude that for large events, plume processes potentially can allow significant CH_4 to escape to the atmosphere from depths of many hundreds of meters. Given the vast estimated CH_4 hydrate (clathrate) reserves below the seafloor, 2×10^{15} g [*Collett and Kuuskraa*, 1998; *Kvenvolden*, 1999], any process that enhances the marine CH_4 contribution to the atmosphere potentially is important to climate change.
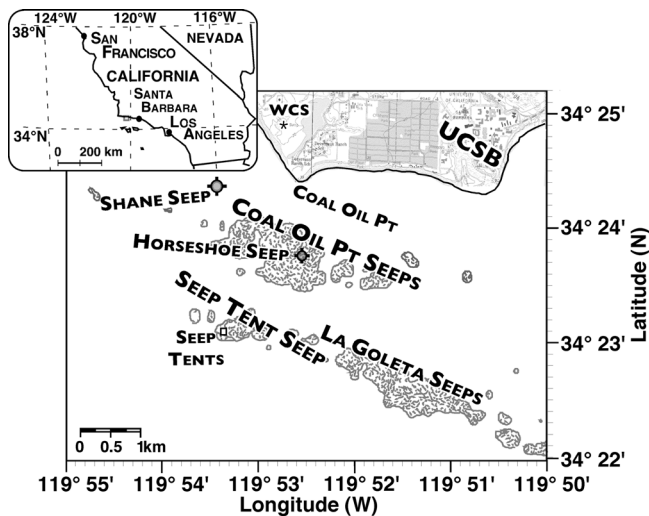
2. Setting

[7] Observations were made at a highly active, shallow (22 m) marine seep area (unofficially named Shane Seep;

---

[1]Marine Sciences Institute, University of California, Santa Barbara, Santa Barbara, California, USA.

[2]Also at Institute for Crustal Studies, University of California, Santa Barbara, Santa Barbara, California, USA.

[3]Earth Science Department, University of California, Santa Barbara, Santa Barbara, California, USA.
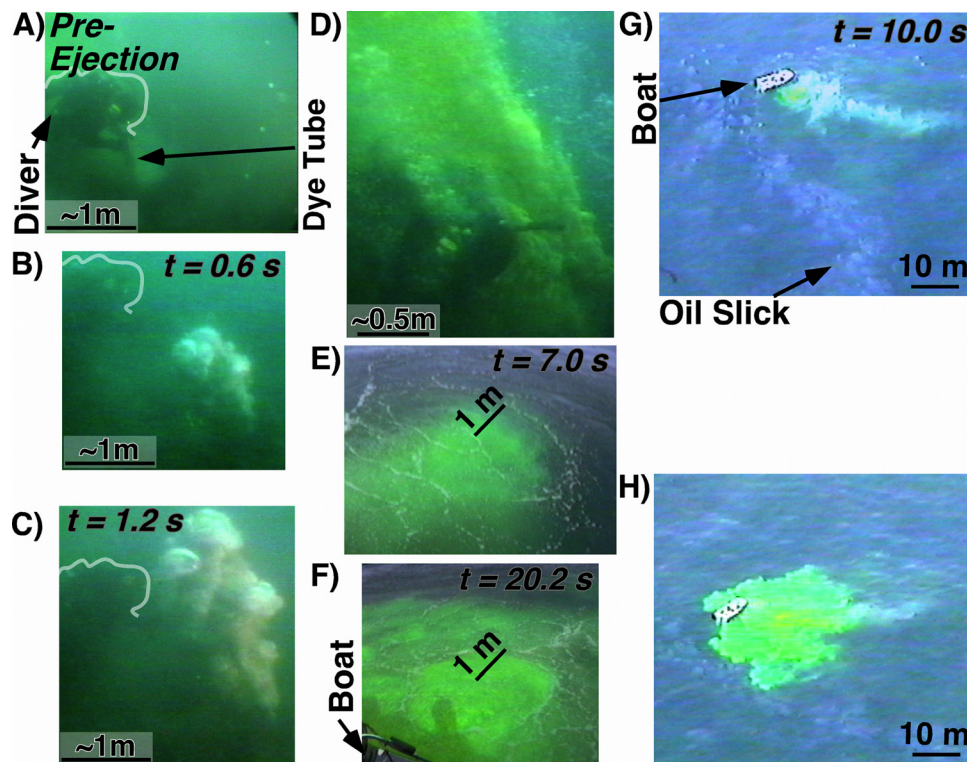
Figure 1. Coal Oil Point seep field, Santa Barbara Channel, California. Gray areas in main panel indicate regions of high bubble density determined from sonar returns [*Hornafius et al.*, 1999]. Inshore seeps were too shallow for sonar surveys. WCS is West Campus air pollution Station, and UCSB is University of California, Santa Barbara.

$34°24.370'N$, $119°53.428'W$) in the Coal Oil Point (COP) seep field, near the University of California, Santa Barbara (Figure 1). The COP seep field releases to the atmosphere 1.15 m^3 gas s^{-1} [*Hornafius et al.*, 1999] and 13,000 L oil day^{-1} (0.00015 m^3 s^{-1}) [*Clester et al.*, 1996] from ~3 km^2 of seafloor. Seepage shows significant temporal variability, on timescales from seconds to decades [*Quigley et al.*, 1999; *Boles et al.*, 2001; *Leifer and Boles*, 2005a, 2005b].
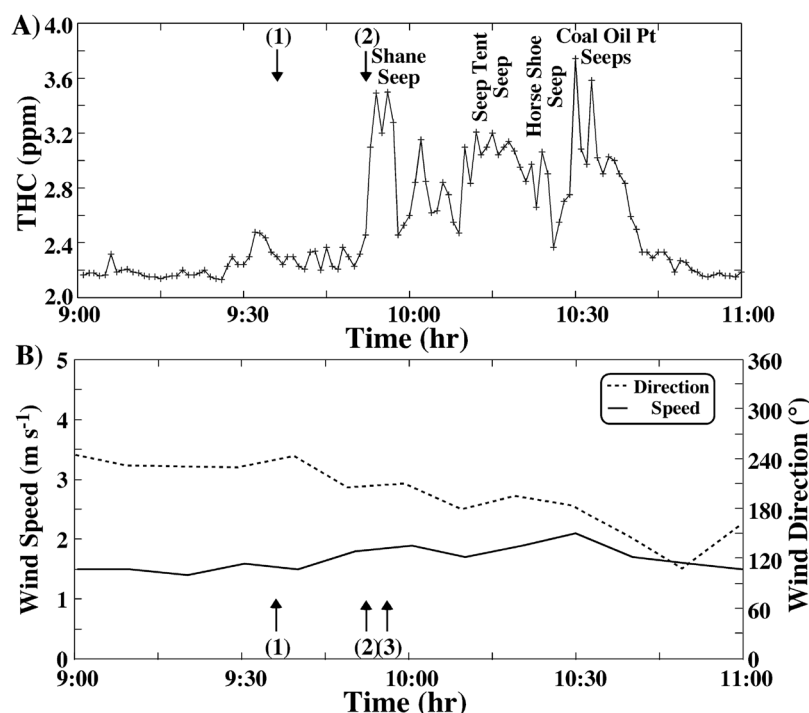
[8] Intense seepage at Shane Seep escapes from vents centered in several pockmark-like hydrocarbon (HC) volcanoes, so termed because of their high tar to sand content ratio [*La Montagne et al.*, 2004]. On 7 November 2002, two heavy iron chains were lain down along N-S and E-W lines that transected a HC volcano, which had formed a few weeks earlier. Several months later, video surveys showed the chain on the seabed except where it penetrated the volcano walls, demonstrating a depositional process for the formation of HC volcano walls. Observations described below suggest chain burial likely occurred from multiple gas blowout events.

3. Observations

[9] On 8 March 2002, SCUBA divers were at Shane Seep to measure the bubble plume's upwelling flow velocity, V_{up},

Figure 2. Video captures of large gas ejection at Shane Seep during a dye injection experiment. (a) Before the ejection, seepage was quiescent. (b) Blowout bubble streams rose and (c) grew rapidly. (d) Seconds later the diver (outlined in white) injected dye. (e) Dye first reached the sea surface 7 s after injection. (f) The main bulk of dye arrived slightly later. (g) Overflight images (boat is 7 m) show initial arrival and (h) after several tens of seconds. Times are relative to blowout. Size scale is on figure.

Figure 3. (a) West Campus air pollution Station (WCS) measurements of total hydrocarbon (THC) and (b) wind speed and wind direction for 8 March 2002. (1) is time of event, (2) is predicted time of arrival of plume, and (3) is the end of the event.

the velocity water moves vertically owing to the rising bubbles, by introducing fluorescein dye into the bubble stream at the seabed and measuring its time of arrival at the sea surface [*Clark et al.*, 2003]. Video cameras were situated at the seabed and 5 m above, at the sea surface, and in an airplane. A test dye release at 0845 Local Time (LT) yielded a 50-s transit time, V_{up} ~44 cm s^{-1}, comparable to previous values [*Clark et al.*, 2003]. Ten minutes before the airplane's arrival, divers reported that seabed seepage at the main HC volcano had virtually ceased (Figure 2a). At 0936 LT a large gas ejection occurred at the seabed (Figures 2b and 2c). Suddenly, three separate gas streams arose from the seabed, described by the divers as sounding like a freight train. The leading bubbles expanded very rapidly to several meters in diameter by 5 m above the seabed. Dye introduced into the bubble flow at the seabed a few seconds after the blowout (Figure 2d) first was observed at the sea surface ~7 s later (Figure 2e), peak V_{up} ~ 300 cm s^{-1}, while the main mass of dye arrived ~10 s after dye injection, V_{up} ~ 200 cm s^{-1}. Bubble plumes lift deeper, cooler water that forms a divergent outward flow of water at the sea surface. During the blowout, the area of outward flow expanded rapidly (Figure 2f). Overflight images showed the dyed bubble stream transversing the water column, tilted by the currents (Figures 2g and 2h). Meanwhile, seabed video showed tar pieces settled between the divers and vents in the area of the volcano walls and the continued emission of very large (>1 cm diameter) bubbles. After several minutes, the flux began decreasing slowly

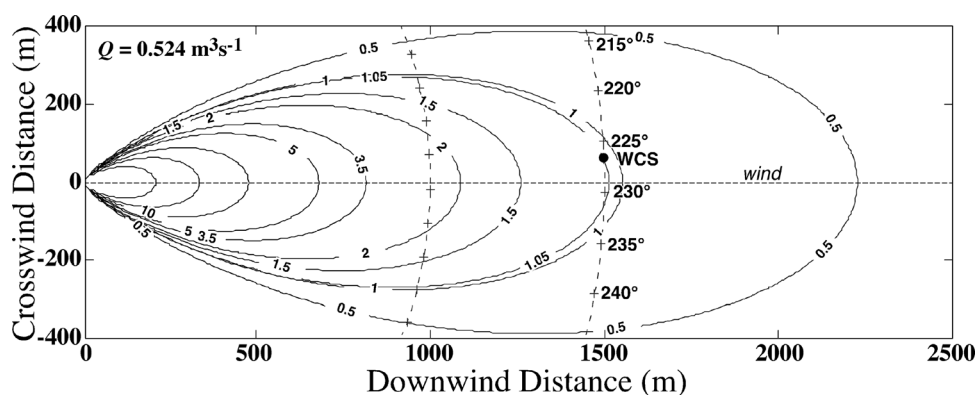until seabed video showed a return to approximately normal emissions.

4. Atmospheric Plume

[10] In the onshore direction (47°) and 1.49 km distant from Shane Seep lies the West Campus air pollution monitoring Station (WCS), ~0.7 km from the shoreline (Figure 1), which records standard meteorological parameters and total hydrocarbon (THC). The wind direction was onshore during the period of the ejection and the plume from the ejection was detected at WCS at precisely the time predicted on the basis of the wind speed.

[11] The mean 10-m wind speed, u, at WCS from 0930 to 0950 LT was 1.57 ± 0.15 m s^{-1} (Figure 3b), yielding an advection time of 15.8 ± 1.6 min and a predicted arrival time of 0952 LT. The recorded THC (Figure 3a) showed a sharp increase at 0952 LT. THC levels were elevated an average 1.05 ppm above background for 6 min. Background was defined as the mean THC prior to the blowout, from 0935 to 0945 LT, and was 2.28 ppm, which is above global background owing to the dispersed input from the seep field. Plumes from other sources in the seep field also pass over WCS. For example, a plume from the Seep Tent Seep area (from 195°, 3.6 km from WCS), the largest concentrated area of seepage within the Coal Oil Point seep field, arrived at 1010 LT when the wind began shifting southward.

[12] Source strength, Q (m^3 s^{-1}), was back-calculated from the WCS THC-data using a Gaussian plume model

Figure 4. Gaussian plume calculation for Case 1 (see text) for a source strength, Q, which yields 1.05 ppm THC at 1.49 km and 227° for wind from 229°. See text for further details of the plume calculation. The location of West Campus Station (WCS) and wind direction are shown on figure. Dashed lines at 1.00 and 1.49 km are from Shane Seep, and contours are ppm THC.

[*Hanna et al.*, 1982] where the downwind surface concentration, C, is

$$C(X, Y) = 2\pi\sigma_Z(X)\sigma_Y(X)Qu \ e^{-\frac{1}{2}\left(\frac{Y}{\sigma_Y(X)}\right)^2} e^{-\frac{1}{2}\left(\frac{Z+h}{\sigma_Z(X)}\right)^2}, \quad (1)$$

where X and Y are the downwind and cross-wind distances from the source, respectively, Z is altitude, σ_Y and σ_Z are the horizontal and vertical standard deviation in the wind, respectively, and h is the emission height. Here h is assumed zero, because although CH_4 is lighter than air, its mixing ratio in the atmospheric plume under normal seepage and wind conditions is small. Both σ_Y and σ_Z are described by functions of X and depend upon atmospheric stability, which in turn depends upon solar insolation, surface roughness, and u.

[13] We assumed u, wind direction, θ, and atmospheric stability were constant between Shane Seep and WCS. Wind veering likely was negligible along the plume trajectory owing to the proximity of WCS to the shoreline and lack of significant topographic features in the vicinity; WCS is just 6 m above sea level. Moreover beach thermals are not significant early in the morning.

[14] The blowout occurred midmorning under a clear sky. Thus two atmospheric stability cases were simulated, "Briggs Turbulence" for slightly unstable conditions with $2 < u < 3$ m s^{-1} and surface roughness typical of the ocean at these wind speeds for light solar insolation (Case 1) and for moderate solar insolation (Case 2).

[15] For Briggs turbulence,

$$\sigma_Y(X) = 0.11X/\sqrt{1 + 10^{-4}X};$$
$$\sigma_Z(X) = 0.08X/\sqrt{1 + 2X10^{-4}X}. \quad (2)$$

[16] Given C and the distance and direction to the source, Q can be estimated from equations (1) and (2). For the calculations, θ was 229° and u was 1.70 m s^{-1}, the mean from 0930 to 1000 LT. For Case 1 and elevation of THC levels by 1.05 ppm above background at WCS, $Q = 0.52$ m^3 s^{-1} (Figure 4). Sensitivity to θ was tested by calculating Q for θ = 226, 232° with variability based on the ±3° accuracy

of anemometer (Model 020C, Met One Instr., Oregon). For θ = 226° and 232°, Q was 0.56 and 0.52 m^3 s^{-1}, respectively. Sensitivity is small because the wind was almost directly toward WCS from Shane Seep. For Case 2, $Q = 0.235$ m^3 s^{-1}, with a similar low sensitivity to θ. Sensitivity to u for a Gaussian plume is linear (for constant stability class); thus uncertainty in Q from u was ~10%. The main uncertainty was associated with stability class, i.e., Case 1 versus Case 2. For the entire blowout event, the total emission, Q_{tot}, was ~160 m^3 or ~70 m^3, for Cases 1 and 2, respectively. In this study, the average Q from the two cases ($Q = 0.4$ m^3 s^{-1} ±25%, or ~120 m^3 for the entire event) is used. During the event, Q was comparable to the entire seep field output, Q, of 1.15 m^3 s^{-1} [*Hornafius et al.*, 1999] and 10 to 15 times the normal Shane Seep Q of 0.038 m^3 s^{-1} [*Washburn et al.*, 2005].

[17] Although Q derived from the WCS measurements is for total hydrocarbons (THC), grab air samples (1-L Tedlar bags) collected immediately over Shane Seep (~30 cm height) for normal seepage (Table 1) indicate that non-methane hydrocarbons were present in negligible concentrations. Thus for this study we use $Q(THC) = Q(CH_4)$.

[18] Q in moles at the seabed must have been larger than at the sea surface due to gas loss by dissolution. Understanding this loss is critical to predicting the impact of seepage CH_4 on the hydrosphere and atmosphere. For gentle isolated bubble seepage, where bubbles are released sporadically or rise in bubble chains, even from shallow seeps like Shane Seep, most of the CH_4 is not directly transported to the atmosphere by bubbles. However, where bubbles are emitted

Table 1. Gas Composition of Grab Air Sample Above Shane Seep[a]

Gas	Atmosphere, %
CH_4	1.91
C_2H_6	unavailable
C_3H_8	0.0033
C_4H_{10}	0.0026
C_5H_{12}	0.0015
C_{6^+}	0.0156

[a]Analysis is courtesy of Leigh Brewer and the Engineering Analysis Center of Southern California Gas Company.

as a plume, or more so from a blowout, plume processes can be significant [*Leifer and Judd*, 2002; *Leifer and Patro*, 2002]. Bubble plumes are regions of concentrated bubbles where the plume fluid properties (dynamic, physical or chemical) are significantly different from that of the surrounding ocean, such as the presence of an upwelling flow of water due to momentum transfer from the rising bubbles.

[19] Bubble plume processes that enhance bubble-mediated CH_4 transport to the sea surface include plume-water saturation that inhibits bubble dissolution, the generation of rapid upwelling flows that decrease transit time across the water column, and broader bubble size distributions, including very large bubbles that lose less gas than smaller bubbles during transit [*Leifer and Judd*, 2002; *Leifer and Patro*, 2002].

[20] Bubble dissolution is driven by the concentration gradient across the bubble interface (based on Henry's Law). Thus an increase in the plume's aqueous CH_4 concentration decreases this gradient, slowing bubble dissolution. An enhanced upwelling flow decreases water column transit time. Also, the hydrostatic pressure decreases faster and as a result, the concentration difference between the bubble and surrounding water decreases faster, lessening loss of gas from the bubble. Larger bubbles have a greater volume, rise more rapidly, and have a higher volume to surface area ratio than smaller bubbles. Thus larger bubbles transport CH_4 to higher in the water column than smaller bubbles [*Leifer and Judd*, 2002; *Leifer and Patro*, 2002].

[21] Both enhanced upwelling flows and larger bubbles were observed during the blowout, while increased plume-water methane concentrations likely also occurred, but were not measured. The relationships between these plume processes and CH_4 loss to the water column ultimately affects the amount of gas released to the atmosphere. These processes were studied with a numerical bubble-propagation model, described below.

5. Numerical Model Description

[22] The numerical bubble-propagation model solves the coupled differential equations that describe the time rate of change of bubble molar content, n, equivalent spherical radius, r, pressure, P, and depth, z, and is described by *Leifer and Judd* [2002] and *Leifer and Patro* [2002]. More recently, the model was improved to include pressure-dependent effects, specifically, compressibility, and pressure-dependant solubility for CH_4. Compressibility was incorporated as a lookup table with depth, which was derived from *McCain* [1973] and applied to the ideal gas law ($PV = n\zeta\mathbf{R}T$) where V is volume, $\mathbf{R}$ is the universal gas constant, and T is the temperature.

[23] Compressibility, ζ, enters the model in two manners, by increasing the initial n of the bubble and in the equation relating changes in the equivalent spherical radius, r, to changes in bubble pressure, P_B, and n. The size change of the bubble is described by

$$\frac{\partial r}{\partial t} = \left\{ \mathbf{R}T \frac{\partial n}{\partial t} - \frac{4\pi r^3}{3} \rho_w g \frac{\partial z}{\partial t} \right\}$$
$$\cdot \left\{ 4\pi r^2 \left(P_A + \rho_w g z + \frac{2\alpha}{r} \right) - \frac{4\pi r^3}{3} \frac{2\alpha}{r^2} \right\}^{-1}, \quad (3)$$

where ρ_W is the density of water, g is the gravitational constant, z is depth, P_A is atmospheric pressure, and α is the surface tension. Equation (3) can be simplified by introducing a factor q, which is defined from the ideal gas law that converts moles into atmospheres, where $q = \mathbf{R}T/V$, and V is bubble volume. In such case, equation (3) becomes

$$\frac{\partial r}{\partial t} = \left\{ q \frac{\partial n}{\partial t} - \rho_w g \frac{\partial z}{\partial t} \right\} \left\{ 3 \left(P_A + \rho_w g z + \frac{4\alpha}{r^2} \right) \right\}^{-1}. \quad (4)$$
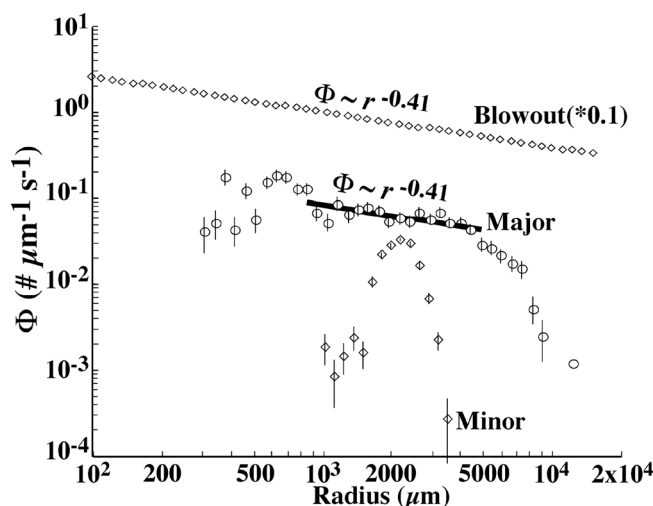
Compressibility is then introduced by defining q^*,

$$q^* = q/\zeta. \quad (5)$$

[24] The model uses a third-fourth-order Runge-Kutta scheme to integrate the differential equations with lookup tables for empirical parameterizations such as the bubble rise velocity, V_B, and the bubble gas-exchange rate, k_B. Both V_B and k_B are parameterized in terms of r among other parameters. In reality, their dependency on r is owing to hydrodynamics of the flow around the bubble. This flow is strongly affected by bubble buoyancy, i.e., r. However, anything that affects the bubble surface state, such as surface-active substances (surfactants) and/or oil, affects bubble hydrodynamics and thus k_B and V_B. Contaminated bubbles have an immobile interface, which causes them to exchange gas slower and rise slower than clean bubbles. Clean bubbles have mobile interfaces. Outside the laboratory, bubbles always have some contamination, which the flow pushes toward the downstream hemisphere. Generally, some portion of the bubble's interface is immobilized (owing to a gradient in surface tension). However, unless the immobile portion of the bubble's interface extends more than 45° from the bubble's downstream pole [*Sadhal and Johnson*, 1983], surfactants have negligible effect on the bubble's behavior and the bubble behaves as if it were clean. The result is that for a given contamination, larger bubbles behave clean, while smaller bubbles behave dirty with a transition between the two behaviors [*Duineveld*, 1995]. This transition has been observed experimentally at $r \sim 500$–700 μm in seawater [*Patro et al.*, 2002] and is used in the model with a transition width of 250 μm.

[25] The model integrates a bubble in each size class from the initial depth and then integrates the solutions over the bubble-emission size distribution, Φ, for each seepage mode. Φ is the number of bubbles in each size class that is emitted at the seabed per second by a seep vent, i.e., the bubble flux. From this, the overall plume gas loss to the water column with respect to depth and to the atmosphere is calculated.

[26] Three different seepage modes were studied, minor, major, and blowout (see Figure 5). Minor vents produce single streams of bubbles with a narrow Φ. Major vents produce a larger and broader Φ than minor vents with bubbles escaping in a jet. The major vent Φ was well described by a power law, $\Phi = Ar^{-0.41}$, where A is a constant [*Leifer et al.*, 2003]. Laboratory studies [*Blanchard and Syzdek*, 1977; *Tsuge et al.*, 1981] and field observations of normal seepage [*Leifer and Boles*, 2005a; *Leifer and MacDonald*, 2003] indicate that high flux (major) vents

Figure 5. Bubble emission size-distributions, Φ, versus bubble radius, r, used in numerical simulations for different seepage modes: a minor plume (stream of solitary bubbles), a major plume (strong upwelling flow) [*Leifer and Boles*, 2005a, 2006], and a blowout plume (labeled on figure). Note that the blowout Φ is multiplied by 0.1. Also shown is the least squares fit to the major plume over the radius range $700-5000$ μm.

produce a broad and weakly size-dependent Φ, which extends to very small and very large bubbles. In contrast, low flux (minor) vents produce a narrow Φ. The power law for the major vent was used for the blowout vent, with Φ ranging from 100 to 15000 μm. A was calculated so that the total CH_4 emission for the blowout from 22 m depth was 0.4 CH_4 m^3 s^{-1} at STP. The upper radius limit for the blowout Φ was estimated from surface visual and seabed video observations, which showed a wide range of bubbles to a few centimeters in diameter.

[27] The model is initialized with the seabed seep gas composition. At the seabed, gas from Shane Seep is primarily CH_4 (83%) and CO_2 (12%) with trace oxygen and nitrogen (2.21%) and nonmethane hydrocarbons (NMHC) decreasing from <3% ethane (Table 2). NMHC were simulated as ethane with a mole fraction of 3%. In the plume, aqueous CH_4 was elevated several orders of magnitude above seep-field background and was only weakly depth dependent: 51.5 and 49.8 μMol L^{-1} at the seabed and sea surface, respectively [*Clark et al.*, 2003].

Unfortunately, water samples were not collected to measure plume CH_4 concentrations for this unanticipated event. However, on the basis of the calculated blowout dissolution a fourth simulation was run for a blowout with elevated plume CH_4, described below. Model output for the minor, major, and blowout simulations are shown in Figure 6.

[28] Model validation was by comparison of predicted and observed sea-surface bubble gas composition for the non-blowout seepage modes (Table 2; minor and major). At the sea surface, bubbles were observed to be composed of CH_4 (78%), air (19.3%), and trace CO_2 (0.6%) and n-alkanes [*Clark et al.*, 2003]. Although CO_2 loss increases the CH_4 mole fraction, air inflow decreases the CH_4 mole fraction. For the minor and major plumes, air in the bubbles at the sea surface was $\sim$5 and 21%, respectively (Table 2). CO_2 outflow was very fast, with just 0.04% and 1.9% remaining at the sea surface, for minor and major, respectively. Mole fractions for the major and minor vent plumes "bracket" the observed sea-surface, bubble mole fractions. This is expected since the surface plume consists of bubble from both the main major vent and the numerous surrounding minor vents. Moreover, the major plume does a better job simulating CO_2, while the minor plume was better for air. Again, this is consistent because soluble gases are more efficiently transported by larger bubbles, which were found almost exclusively in the major plume.

[29] CH_4 loss was greatest for the minor plume, about half of the seabed emission, while the major plume only lost $\sim$10%. However, for the blowout, CH_4 loss was just 1.11%. For the blowout simulation, the sea-surface CH_4 mole-fraction was less than for the major plume, which is explained by the decreased CO_2 outflow and air inflow.

6. Estimation of Blowout Plume Elevation

[30] To test the significance of enhanced dissolved CH_4 in the plume, a fourth simulation was run for plume CH_4 based on the blowout simulation. For the blowout, total gas loss during transit of the water column was 1.11% of the seabed emission of 17.0 moles s^{-1}, i.e., 0.19 moles dissolved. On the basis of the sea-surface, midwater, and seabed observations, we assumed a conical blowout plume, 1 m diameter at the sea surface (Figure 2f) and 22 m tall (volume of 23 m^3). For this plume, plume CH_4 concentrations would have been elevated $\sim$8 μmol L^{-1} above normal. This is conservative

Table 2. Model-Predicted Bubble Gas Mole Fraction at the Sea Surface (1 m Depth), Model Conditions, and Bubble Gas Observations for Shane Seep Main Plume[a,b,c]

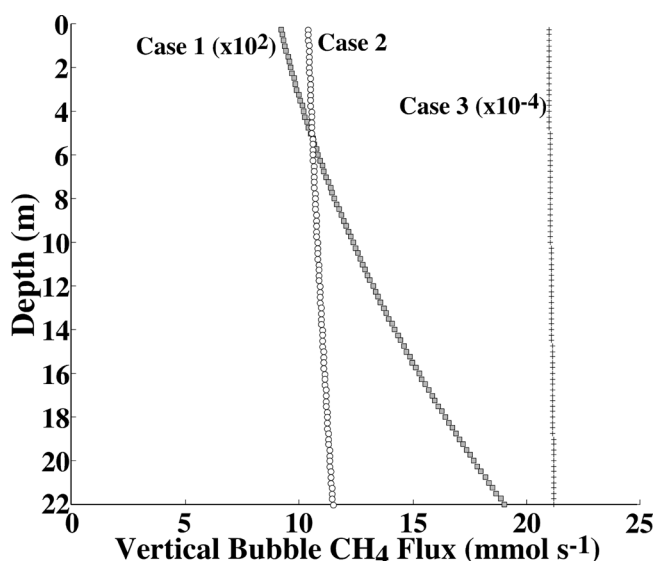|	Gas Flux, mmol s^{-1}	[CH_4], μmol L^{-1}	V_{up}, cm s^{-1}	O_2, %	N_2, %	CH_4, %	CO_2, %	CH_4 Loss, %
Minor bubble	0.19[b]	50	10[b]	5.9	14.9	76.0	0.04	51.6
Major bubble	9.3[c]	50	45[b]	1.2	3.7	89.6	1.9	9.46
Blowout bubble	2.1×10^4[d]	50	200	0.44	2.1	84.7	9.4	1.11
Sampled gas at seabed				0.34	1.9	83	12	
Sampled gas at surface				5.3	14	78	0.6	

[a]Remaining bubble composition: nonmethane hydrocarbons.
[b]From *Leifer and Boles* [2005a].
[c]From *Leifer and Boles* [2006].
[d]Derived from calculated Q for blowout. [CH_4] is aqueous CH_4, and V_{up} is upwelling velocity.

Figure 6. Predicted vertical CH_4 transport (in bubbles) for the three simulations. See Table 1 and text for details. Note that minor plume and blowout simulations are multiplied by 10^2 and 10^{-4}, respectively.

as it neglects plume loss to the bulk ocean, which would lead to lower enhancement of CH_4.

[31] A simulation with plume concentrations elevated by 8 μmol L^{-1} (i.e., 58 μmol L^{-1}) showed negligible difference in terms of methane dissolution from the non-elevated blowout simulation. In fact, a sensitivity study where plume concentrations were elevated by 100 μmol L^{-1} (i.e., 150 μmol L^{-1}) also showed negligible difference from the blowout simulation, 1.096% lost versus 1.107% dissolved. The effect was small because 150 μmol L^{-1} CH_4 is $\sim$5% of CH_4 saturation mid water-column.

[32] Thus for the blowout from this very shallow seep, the primary factor enhancing CH_4 transport to the atmosphere was the rapid upwelling flow. There simply was insufficient time for the plume water to become significantly saturated. A simulation of the blowout event with $V_{up} = 10$ cm s^{-1} lost approximately 7 times the loss of the simulation using the observed $V_{up} = 200$ cm s^{-1}. Also, the presence of very large bubbles with their greater volume significantly aided CH_4 transport; bubbles larger than 5000 μm transported 75% of the CH_4.

[33] For deeper blowout seepage, CH_4 loss increases. Simulating the blowout from 250 m depth showed greater, but still small CH_4 loss, $\sim$9% of the initial CH_4. For comparison, the major vent plume at 250 m lost $\sim$66% of its original CH_4 and the minor plume 100%. Thus if a seep blowout of comparable magnitude occurred at even greater depths (near the hydrate stability depth) and generated similarly strong upwelling flows, a significant fraction of its CH_4 potentially can reach the atmosphere.

7. Discussion

[34] This study presented the first quantitative observation of a blowout or eruptive emission from natural marine

seepage. However, although emissions during the event were significantly elevated, prior to the eruption emissions were observed to stop at the vent site (observations during a scuba dive 1 hour earlier showed normal emissions at the seabed). Thus overall emissions for the event may or may not have been greater. In fact, *Leifer and Boles* [2005b] concluded that for a much smaller ejective event at Shane Seep, the main impact of the ejection was after the event when flux was elevated above normal for a significant time period. This was interpreted as due to the ejection having reduced resistance within the seepage pathway(s). Thus it is unclear if blowout seepage increases overall seepage, or (in a time and spatially averaged sense) is a zero sum effect. Instead, the significance of blowout emissions was the plume processes that allowed much more of the emitted methane to reach higher within the water column and to the atmosphere than for normal seepage. As a result, blowout seepage may allow geologic methane from seeps at depths that normally do not reach the atmosphere to contribute to atmospheric budgets.

[35] The model's conclusions strongly suggest that bubble-mediated CH_4 transport is enhanced significantly for a blowout event. The results suggest that deep blowout-seepage transports CH_4 much higher into the water column than normal seepage. Even for seeps much deeper than those addressed in this study, a significant fraction of blowout seepage methane should reach the winter-mixed layer. For example, under normal seepage, acoustic data shows normal seep bubble plumes can persist for many hundreds to more than 1000 m [*Merewether et al.*, 1985; *Sauter et al.*, 2005]. The methane from these plumes that reaches the winter-mixed layer (which is a few hundred meters deep in areas such as the North Atlantic) likely diffuses across the air-sea interface to the atmosphere, because microbial oxidation timescales are longer than mixing times in the upper ocean layer [*Rehder et al.*, 1999].

[36] It must be noted that the model includes various simplifications. For example, one model simplification is that ambient conditions were assumed constant across the water column. Likewise, the upwelling flow may vary within the water column, decreasing as the plume rises. The plume radius at Shane Seep increased only 50 cm over its 22-m rise, a spreading angle of 1.3°. Had it spread more rapidly the upwelling flow would have decreased, perhaps significantly.

[37] Moreover, the efficiency with which the plume transports methane should increase with the blowout magnitude. Thus larger blowouts with greater upwelling flows should transfer gas more efficiently than smaller events. A striking example was the blowout at the Haltenbanken platform, offshore mid-Norway from 240 m [*Hovland and Judd*, 1988]. The resultant plume reached the sea surface still compact and very intense. This indicates that strong upwelling flows were coherent throughout the water column.

[38] For hydrocarbon seeps like Shane Seep, blowouts likely result from tar blockage that is then blown clear by an increase in pressure [*Hovland*, 2002; *Leifer and Boles*, 2005a]. Deposition of some tar on the HC volcano walls was observed in the video and suggests that burial of the

chain here was by multiple blowout events. Seafloor pockmarks, concave crater-like depressions that are common seepage-related features on all continental shelves, are proposed to result from an explosive formation process [*Hovland et al.*, 2002]. If other pockmarks are formed by (nontar) blowout mechanisms, then blowout seepage may occur sufficiently frequently to contribute significantly to atmospheric CH_4 budgets.

[39] Dead carbon (^{14}C depleted) methane contributes $\sim$110 $\pm$ 45 Tg yr^{-1} to the atmosphere [*Crutzen and Lelieveld*, 2001] and arises from coalmines, leaking gas lines, natural gas hydrate decomposition and geologic sources. Geologic sources contribute an estimated 16– 70 Tg yr^{-1} [*Etiope and Klusman*, 2002; *Judd et al.*, 2002]. *Kvenvolden and Rogers* [2005] have argued that the geologic source strength of ^{14}C-depleted CH_4 is 45 Tg yr^{-1} of which macro seeps such as discussed herein are the major component. One prominent source of geologic CH_4 is eruption from mud volcanoes [*Dimitrov*, 2002; *Kopf*, 2003]. Many mud volcanoes have been surveyed in the marine realm [*Milkov*, 2000]. Eruptions from these sources along with the sudden dissociation of marine methane hydrates could be another (abrupt) source of geologic CH_4 to the atmosphere.

8. Conclusions

[40] Our study here suggests that the rate of discharge is an important factor in determining whether CH_4 released from ocean depths beyond the continental shelves can reach the atmosphere. The answer is likely controlled by the magnitude of the sudden discharge, which if large enough will allow transport of CH_4 to the sea surface with minimal dissolution in the ocean. This may be significant both to understanding past rapid climate changes [*Kennett et al.*, 2003; *Severinghaus et al.*, 1998], but also the implications of warmer future oceans [*Archer and Buffett*, 2005].

[41] This study was possible owing to several fortuitous circumstances including wind that advected the seep plume to an air pollution measurement station, which allowed the back calculation of the source strength. Moreover, the results suggest the importance of large transient emissions that owing to plume processes allow the CH_4 to reach far shallower depths in the ocean than for significantly smaller, continuous emissions. However, assessment of the blowout contribution requires knowledge of the frequency and magnitude of such events. One approach to address this would be deployment of a measurement station in the prevailing downwind direction from the target seep area. Another approach would be the long-term deployment of a seabed monitoring station near a seep area. Such a station might include a turbine tent [*Leifer and Boles*, 2005b] specifically designed to respond to the high flow rates during a blowout and include a sea-surface monitoring station to record the arrival time of colder, deeper water. Other approaches could include a side-viewing sonar monitor installed at the seafloor.

[42] This research presented the first quantitative estimates of methane transport from the seafloor to the atmosphere from a blowout seepage event. During blowout seepage, vertical methane-transport efficiency is enhanced so that virtually all the methane from a shallow seep reaches the atmosphere. A model study suggests that given sufficient blowout size and resultant upwelling flow, efficient methane transport to the sea surface could occur from depths of hundreds of meters or greater, possibly near the depths of the hydrate stability boundary. Therefore we suggest that our present study has identified a process that enables rapid climate change by massive methane bubble releases from sudden decomposition of hydrates.

[43] Long-term monitoring of seeps to quantify blowout characteristics (upwelling flow velocities, bubble plume size distributions, and plume aqueous concentrations) will be required to provide data for accurate modeling. Also needed is an understanding of the frequency and magnitudes of these events. Blowout emissions allow methane to transit the water column from great depth, implying that the marine seep contribution to atmospheric methane budgets likely is underestimated.

References

Archer, D., and B. Buffett (2005), Time-dependent response of the global ocean clathrate reservoir to climatic and anthropogenic forcing, *Geochem. Geophys. Geosyst.*, *6*, Q03002, doi:10.1029/2004GC000854.

Blanchard, D. C., and L. D. Syzdek (1977), Production of air bubbles of a specified size, *Chem. Eng. Sci.*, *32*, 1109–1112.

Boles, J. R., J. F. Clark, I. Leifer, and L. Washburn (2001), Temporal variation in natural methane seep rate due to tides, Coal Oil point area, California, *J. Geophys. Res.*, *106*(C11), 27,077–27,086.

Clark, J. F., I. Leifer, L. Washburn, and B. P. Luyendyk (2003), Compositional changes in natural gas bubble plumes: Observations from the Coal Oil Point marine hydrocarbon seep field, *Geo Mar. Lett.*, *23*, 187–193, doi:10.1007/s00367-003-0137-y.

Clester, S. M., J. S. Hornafius, J. Scepan, and J. E. Estes (1996), Quantification of the relationship between natural gas seepage rates and surface oil volume in the Santa Barbara Channel (abstract), *Eos Trans. AGU*, *77*(46), Fall Meet Suppl., F419.

Collett, T. S., and V. A. Kuuskraa (1998), Emerging US gas resources: 4. Hydrates contain vast store of world's gas resources, *Oil Gas J.*, *96*(19), 90–95.

Crutzen, P. J., and J. Lelieveld (2001), Human impacts on atmospheric chemistry, *Annu. Rev. Earth Planet. Sci.*, *29*, 17–45.

Dickens, G. R., J. R. O'Niel, D. K. Rea, and R. M. Owen (1995), Dissociation of oceanic methane hydrate as a cause of the carbon isotope excursion at the end of the Paleocene, *Paleoceanography*, *10*, 965–971.

Dimitrov, L. I. (2002), Mud volcanoes—The most important pathways for degassing deeply buried sediments, *Earth Sci. Rev.*, *59*, 49–76.

Duineveld, P. C. (1995), The rise velocity and shape of bubbles in pure water at high Reynolds number, *J. Fluid Mech.*, *292*, 325–332.

Etiope, G., and R. W. Klusman (2002), Geologic emissions of methane to the atmosphere, *Chemosphere*, *49*(8), 777–789.

Hanna, S. R., G. A. Briggs, and H. J. R. P. (1982), *Handbook on Atmospheric Diffusion*, edited by J. Smith, Tech. Inf. Cent., U.S. Dep. of Energy, Washington, D. C.

Heeschen, K. U., A. M. Tréhu, R. W. Collier, E. Suess, and G. Rehder (2003), Distribution and height of methane bubble plumes on the Casca-

dia Margin characterized by acoustic imaging, *Geophys. Res. Lett.*, *30*(12), 1643, doi:10.1029/2003GL016974.

Hornafius, J. S., D. C. Quigley, and B. P. Luyendyk (1999), The world's most spectacular marine hydrocarbons seeps (Coal Oil Point, Santa Barbara Channel, California): Quantification of emissions, *J. Geophys. Res.*, *104*(C9), 20,703–20,711.

Hovland, M. (2002), On the self-sealing nature of marine seeps, *Cont. Shelf Res.*, *22*, 2387–2394.

Hovland, M., and A. G. Judd (1988), *Seabed Pockmarks and Seepage: Impact on Geology, Biology, and the Marine Environment*, 293 pp., Graham and Trotman, Boston, Mass.

Hovland, M., J. Gardner, and A. Judd (2002), The significance of pockmarks to understanding fluid flow processes and geohazards, *Geofluids*, *2*, 127–136.

Intergovernmental Panel on Climate Change (2001), *Climate Change 2001—The Scientific Basis*, 881 pp., Cambridge Univ. Press, New York.

Judd, A. G., M. Hovland, L. I. Dimitrov, S. Garcia Gil, and V. Jukes (2002), The geological methane budget at continental margins and its influence on climate, *Geofluids*, *2*, 109–126.

Katz, M. E., D. K. Pak, G. R. Dickens, and K. G. Miller (1999), The source and fate of massive carbon input during the latest Paleocene Thermal Maximum, *Science*, *286*, 1531–1533.

Kennett, J. P., K. G. Cannariato, I. L. Hendy, and R. J. Behl (2003), *Role of Methane Hydrates in Late Quaternary Climatic Change: The Clathrate Gun Hypothesis*, *Spec. Publ.*, vol. 54, 216 pp., AGU, Washington, D. C.

Khalil, M. A. K., and R. A. Rasmussen (1995), The changing composition of the Earth's atmosphere, in *Composition, Chemistry, and Climate of the Atmosphere*, edited by H. B. Singh, pp. 50–87, Van Nostrand Reinhold, Hoboken, N. J.

Kopf, A. J. (2003), Global methane emission through mud volcanoes and its past and present impact on the Earth's climate, *Int. J. Earth Sci.*, *2*(5), 806–816, doi:10.1007/s00531-003-0341-z.

Kvenvolden, K. A. (1999), Potential effects of gas hydrate on human welfare, *Proc. Natl. Acad. Sci. U. S. A.*, *96*(7), 3420–3426.

Kvenvolden, K. A., and B. W. Rogers (2005), Gaia's Breath—Global methane exhalations, *Mar. Pet. Geol.*, *22*(4), 579–590.

Kvenvolden, K. A., T. D. Lorenson, and W. S. Reeburgh (2001), Attention turns to naturally occurring methane seepage, *Eos Trans. AGU*, *82*(40), 457.

La Montagne, G., I. Leifer, S. Bergmann, L. C. Van De Werfhorst, and P. A. Holden (2004), Bacterial diversity in marine hydrocarbon-seep sediments, *Environ. Microbiol.*, *6*(8), 799–808.

Leifer, I., and J. R. Boles (2005a), Measurement of marine hydrocarbon seep flow through fractured rock and unconsolidated sediment, *Mar. Pet. Geol.*, *22*(4), 551–568.

Leifer, I., and J. R. Boles (2005b), Turbine tent measurements of marine hydrocarbon seeps on subhourly time scales, *J. Geophys. Res.*, *110*, C01006, doi:10.1029/2003JC002207.

Leifer, I., and J. R. Boles (2006), Corrigendum to: Measurement of marine hydrocarbon seep flow through fractured rock and unconsolidated sediment, *Mar. Pet. Geol.*, in press.

Leifer, I., and A. G. Judd (2002), Oceanic methane layers: A bubble deposition mechanism from marine hydrocarbon seepage, *Terra Nova*, *16*, 471.

Leifer, I., and I. R. MacDonald (2003), Dynamics of the gas flux from shallow gas hydrate deposits: Interaction between oily hydrate bubbles and the oceanic environment, *Earth Planet. Sci. Lett.*, *210*, 411–424.

Leifer, I., and R. K. Patro (2002), The bubble mechanism for methane transport from the shallow sea bed to the surface: A review and sensitivity study, *Cont. Shelf Res.*, *22*, 2409–2428.

Leifer, I., G. De Leeuw, and L. H. Cohen (2003), Optical measurement of bubbles: System, design and application, *J. Atmos. Oceanic Technol.*, *20*(9), 1317–1332.

Loseth, H., L. Wensaas, B. Arntsen, N. Hanken, C. Basire, and K. Graue (2001), 1000 m long gas blow-out pipes, paper presented at EAGE 63rd Conference and Technical Exhibition, Eur. Assoc. of Geophys. and Eng., Amsterdam, Netherlands.

MacDonald, I. R., I. Leifer, R. Sassen, P. Stine, R. Mitchell, and J. R. Guinasso (2002), Transfer of hydrocarbons from natural seeps to the water column and atmosphere, *Geofluids*, *2*, 95–107.

McCain, W. D., Jr. (1973), *Properties of Petroleum Physics*, Penwell, Tulsa Okla.

Merewether, R., M. S. Olsson, and P. Lonsdale (1985), Acoustically detected hydrocarbon plumes rising from 2-km depths in Guaymas Basin, Gulf of California, *J. Geophys. Res.*, *90*(4), 3075–3085.

Milkov, A. (2000), Worldwide distribution of submarine mud volcanoes and associated gas hydrates, *Mar. Geol.*, *167*, 29–42.

Norris, R. D., and U. Röhl (1999), Carbon cycling and chronology of climate warming during the Palaeocene/Eocene transition, *Nature*, *401*, 775–778, doi:10.1038/44545.

Patro, R., I. Leifer, and P. Bowyer (2002), Better bubble process modeling: Improved bubble hydrodynamics parameterization, in *Gas Transfer and Water Surfaces*, *Geophys. Monogr. Ser.*, vol. 127, edited by M. Donelan et al., pp. 315–320, AGU, Washington, D. C.

Prather, M., R. Derwent, D. Ehhalt, P. Fraser, E. Sanhueza, and X. Zhou (1995), Other trace gases and atmospheric chemistry, in *Climate Change 1994: Radiative Forcing of Climate Change and an Evaluation of the IPCC IS92 Emission Scenarios*, edited by J. T. Houghton et al., pp. 73–126, Cambridge Univ. Press, New York.

Quigley, D. C., J. S. Hornafius, B. P. Luyendyk, R. D. Francis, J. F. Clark, and L. Washburn (1999), Decrease in natural marine hydrocarbon seepage near Coal Oil Point, California, associated with offshore oil production, *Geology*, *27*(11), 1047–1050.

Reeburgh, W. S. (2003), Global methane biogeochemistry, in *The Atmosphere*, edited by R. Keeling, pp. 65–69, Elsevier, New York.

Rehder, G., R. S. Keir, E. Suess, and M. Rhein (1999), Methane in the northern Atlantic controlled by microbial oxidation and atmospheric history, *Geophys. Res. Lett.*, *26*(5), 587–590.

Rowland, F. S. (1985), Methane and chlorocarbons in the Earth's atmosphere, *Origins Life Evol. Biosphere*, *15*, 279–298.

Sadhal, S., and R. E. Johnson (1983), Stoke's flow past bubbles and drops partially coated with thin films, *J. Fluid Mech.*, *126*, 237–250.

Sauter, E. J., S. I. Muyakshin, J.-L. Charlou, M. Schlüter, A. Boetius, K. Jerosch, E. Damm, J.-P. Foucher, and M. Klages (2005), Methane discharge from a deep-sea submarine mud volcano into the upper water column by gas hydrate-coated methane bubbles, *Earth Planet. Sci. Lett.*, *243*, 354–365.

Severinghaus, J. P., T. Sowers, E. J. Brook, R. B. Alley, and M. L. Bender (1998), Timing of abrupt climate change at the end of the Younger Dryas interval from thermally fractionated gases in polar ice, *Nature*, *391*, 141–146, doi:10.1038/34346.

Tsuge, H., S. Hibino, and U. Nojima (1981), Volume of a bubble formed at a single submerged orifice in a flowing liquid, *Int. J. Chem. Eng.*, *21*, 630.

Valentine, D. L., D. C. Blanton, W. S. Reeburgh, and M. Kastner (2001), Water column methane oxidation adjacent to an area of active hydrate dissociation, Eel River Basin, *Geochim. Cosmochim. Acta*, *65*, 2633–2640.

Washburn, L., J. F. Clark, and P. Kyriakidis (2005), The spatial scales, distribution, and intensity of natural marine hydrocarbon seeps near Coal Oil Point, California, *Mar. Pet. Geol.*, *22*(4), 569–578.

Watanabe, S., N. Tsurushima, M. Kusakabe, and S. Tsunogai (1995), Methane in Izena Cauldron, Okinawa Trough, *J. Oceanogr.*, *51*, 239.

———————

J. Boles, J. F. Clark, and B. P. Luyendyk, Earth Science Department, University of California, Santa Barbara, Santa Barbara, CA 93106, USA.

I. Leifer, Marine Sciences Institute, University of California, Santa Barbara, Santa Barbara, CA 93106, USA. (ira.leifer@bubbleology.com)